Tokyo Climate Center, Japan Meteorological Agency

TCC News

No. 34 Autumn 2013

Contents

El Niño Outlook (October 2013 – April 2014)

ENSO-neutral conditions are likely to continue during the Northern Hemisphere autumn and winter.

El Niño/La Niña

In September 2013, the NINO.3 sea surface temperature (SST) was near normal with a deviation of -0.2°C. SSTs (Figures 1 and 3 (a)) and subsurface temperatures (Figures 2 and 3 (b)) were above normal in the western equatorial Pacific, while easterly winds in the lower troposphere were stronger than normal in the central part. Meanwhile, deviations from the normals of SSTs and subsurface ocean temperatures were small in the central and eastern equatorial Pacific. This means that La Niña-like conditions, which had been observed during the Northern Hemisphere summer, weakened in September, and ENSO-neutral conditions continued in the equatorial Pacific.

According to JMA's El Niño prediction model, the NINO.3 SST will be near normal during the forecast period (Figure 4). As subsurface ocean temperature anomalies in the central and eastern equatorial Pacific were small, SSTs in the eastern part are not expected to be significantly affected by subsurface ocean conditions in the months ahead. In conclusion, it is likely that ENSO-neutral conditions will continue during the Northern Hemisphere autumn and winter.

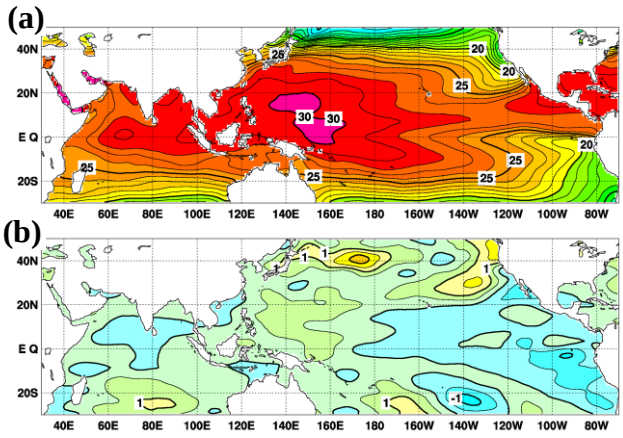

Figure 1 Monthly mean (a) sea surface temperatures (SSTs) and (b) SST anomalies in the Indian and Pacific Ocean areas for September 2013
The contour intervals are 1˚C in (a) and 0.5˚C in (b). The base period for the normal is 1981 – 2010.

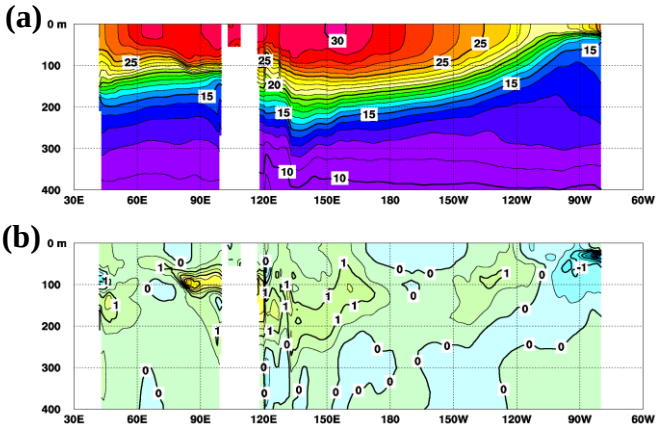

Figure 2 Monthly mean depth-longitude cross sections of (a) temperatures and (b) temperature anomalies in the equatorial Indian and Pacific Ocean areas for September 2013
The contour intervals are 1˚C in (a) and 0.5˚C in (b). The base period for the normal is 1981 – 2010.

Western Pacific and Indian Ocean

The area-averaged SST in the tropical western Pacific (NINO.WEST) region was above normal in September. It is likely to approach normal in the months ahead, and to be near normal during the Northern Hemisphere winter.

The area-averaged SST in the tropical Indian Ocean (IOBW) region was near normal in September. It is likely to be near or below normal during the Northern Hemisphere autumn and winter.

(Ichiro Ishikawa, Climate Prediction Division)

* The SST normal for NINO.3 region (5°S – 5°N, 150°W – 90°W) is defined as the monthly average over a sliding 30-year period (1983-2012 for this year).
* The SST normals for the NINO.WEST region (Eq. – 15°N, 130°E – 150°E) and the IOBW region (20°S – 20°N, 40°E – 100°E) are defined as linear extrapolations with respect to a sliding 30-year period, in order to remove the effects of significant long-term warming trends observed in these regions.

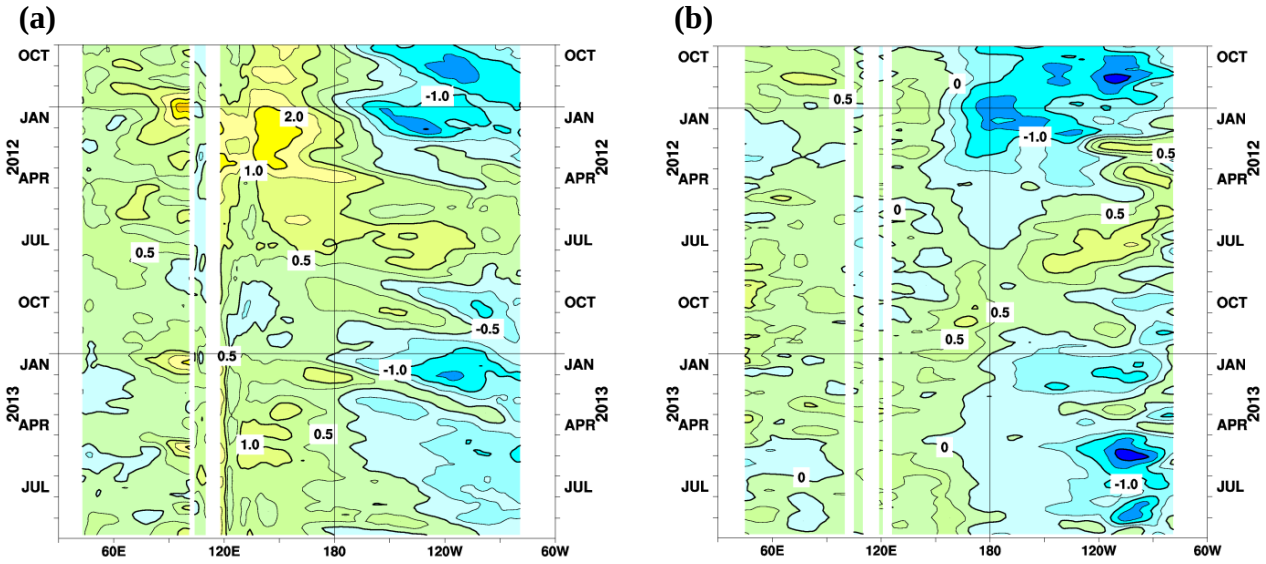

Figure 3 Time-longitude cross sections of (a) SST and (b) ocean heat content (OHC) anomalies along the equator in the Indian and Pacific Ocean areas

OHCs are defined here as vertical averaged temperatures in the top 300 m. The base period for the normal is 1981 – 2010.

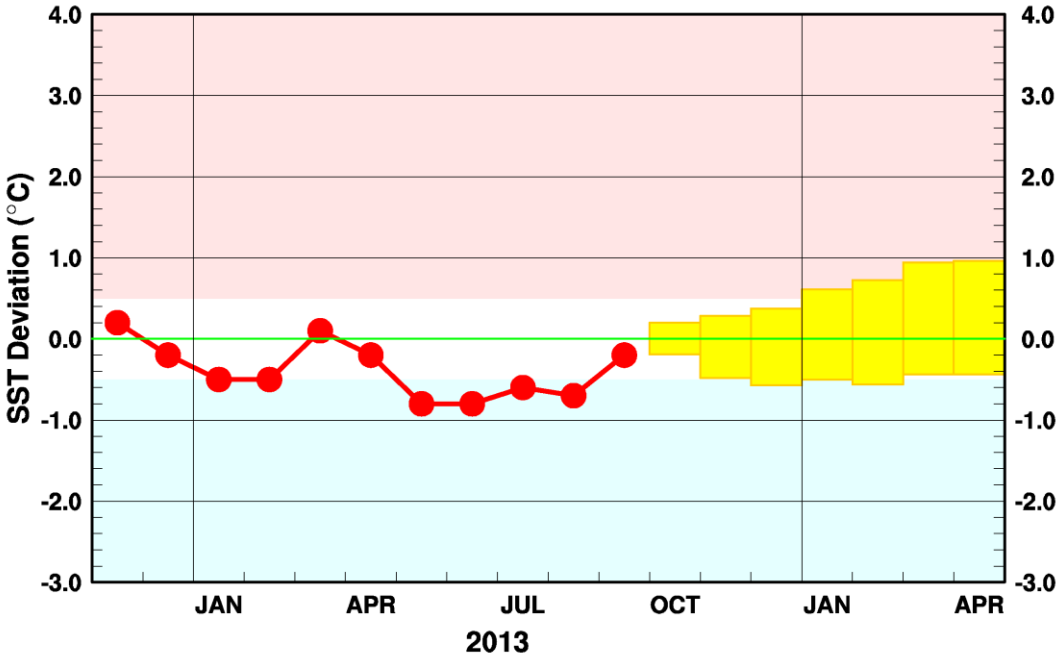

Figure 4 Outlook of NINO.3 SST deviation produced by the El Niño prediction model

This figure shows a time series of monthly NINO.3 SST deviations. The thick line with closed circles shows observed SST deviations, and the boxes show the values produced for the next six months by the El Niño prediction model. Each box denotes the range into which the SST deviation is expected to fall with a probability of 70%.

JMA's Seasonal Numerical Ensemble Prediction for Winter 2013/2014

Based on JMA's seasonal ensemble prediction system, active convection is expected over the western tropical Pacific in winter 2013/2014. In association, the sub-tropical jet stream is expected to shift northward over the eastern part of the Eurasian Continent and air temperatures are expected to be above normal around Southeast Asia. Conversely, the sub-tropical jet stream is expected to shift southward from East Asia to the east of Japan and the Aleutian Low is expected to shift westward, suggesting a stronger-than-normal East Asian winter monsoon.

1. Introduction

This article outlines JMA's dynamical seasonal ensemble prediction for winter 2013/2014 (December 2013 – February 2014, referred to as DJF), which was used as a basis for the Agency's operational cold-season outlook issued on 24 October, 2013. The outlook detailed here is based on the seasonal ensemble prediction system of the Coupled atmosphere-ocean General Circulation Model (CGCM). See the column below for system details.

Section 2 outlines global SST anomaly predictions, and Section 3 describes the associated circulation fields expected over the tropics and sub-tropics. Finally, the circulation fields predicted for the mid- and high latitudes of the Northern Hemisphere are discussed in Section 4.

2. SST anomalies (Figure 5)

Figure 5 shows predicted SSTs and related anomalies for DJF. Above-normal values are expected in the western tropical Pacific, while below-normal values are expected from central to eastern parts of the equatorial Pacific.

3. Prediction for the tropics and sub-tropics (Figure 6)

Figure 6 (a) shows predicted precipitation and related anomalies for DJF. Precipitation is expected to be above normal from the western tropical Pacific to the northern part of the Indian Ocean. However, the results of hindcast experimentation indicate that the level of prediction skill for precipitation over the northern part of the Indian Ocean is relatively low in the tropics. Accordingly, the prediction of above-normal precipitation over the northern part of the Indian Ocean should not be relied on too heavily.

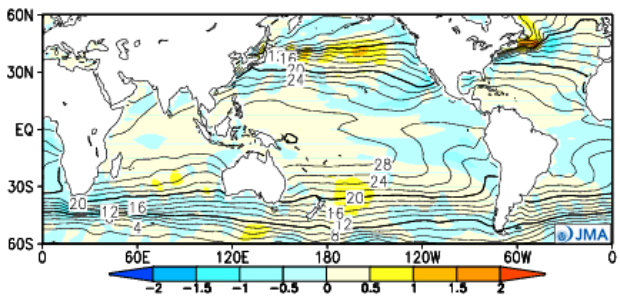

Figure 5 Predicted SSTs (contours) and SST anomalies (shading) for December 2013 – February 2014 (ensemble mean of 51 members)
The contour interval is 2°C.

(a)Precipitation

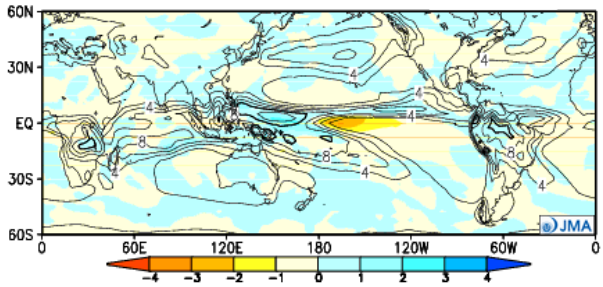

(b)CHI200

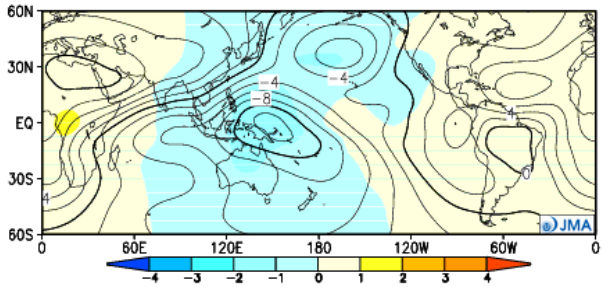

(c)PSI200

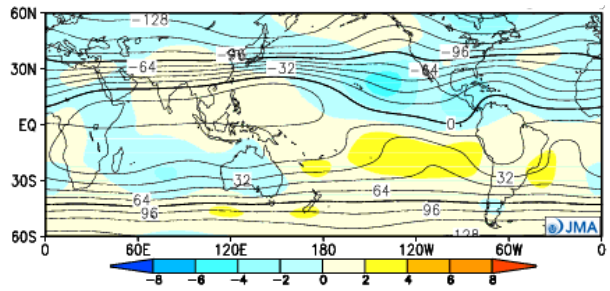

(d)Tsurf

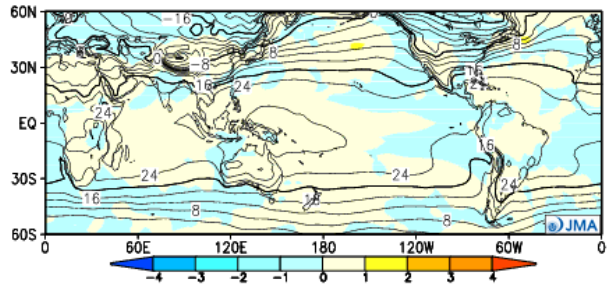

Figure 6 Predicted atmospheric fields from 60°N – 60°S for December 2013 – February 2014 (ensemble mean of 51 members)
(a) Precipitation (contours) and anomaly (shading). The contour interval is 2 mm/day.
(b) Velocity potential at 200 hPa (contours) and anomaly (shading). The contour interval is 2×10^6 m^2/s.
(c) Stream function at 200 hPa (contours) and anomaly (shading). The contour interval is 16×10^6 m^2/s.
(d) Surface air temperature (contours) and anomaly (shading). The contour interval is 4°C.

Velocity potential in the upper troposphere (200 hPa) (Figure 6 (b)) is expected to be negative (i.e., more divergent) from the western tropical Pacific to the eastern part of the Indian Ocean, reflecting active convection in the former. Conversely, positive (i.e., more convergent) anomalies are predicted from central to eastern parts of the equatorial Pacific.

The stream function at 200 hPa (Figure 6 (c)) is expected to be positive (i.e., anti-cyclonic) from South to Southeast Asia, which may be related to active convection from the western tropical Pacific. In association, the sub-tropical jet stream is expected to shift northward over the eastern part of the Eurasian Continent and above-normal air temperatures are expected over Southeast Asia (Figure 6 (d)). Conversely, negative (i.e., cyclonic) anomalies are expected from East Asia to the east of Japan, suggesting that the sub-tropical jet stream may shift southward over the region.

4. Prediction for the mid- and high latitudes of the Northern Hemisphere (Figure 7)

Around the Aleutian Low region, anomalies of sea level pressure (SLP) (Figure 7 (a)) and 500-hPa geopotential height (Figure 7 (b)) are expected to be positive on the eastern side and negative on the western side, suggesting that the Aleutian Low may shift westward. The East Asian winter monsoon is therefore expected to be stronger than normal over East Asia. of Japan, suggesting that the sub-tropical jet stream is expected to shift southward over the region.

(Masayuki Hirai, Climate Prediction Division)

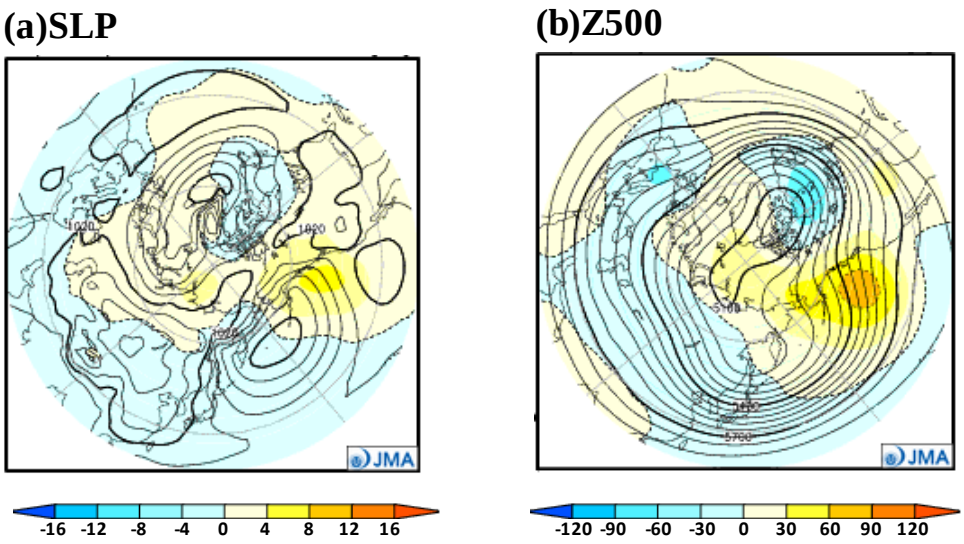

Figures 7 Predicted atmospheric fields from 20°N – 90°N for December 2013 – February 2014 (ensemble mean of 51 members)
(a) Sea level pressure (contours) and anomaly (shading). The contour interval is 4 hPa.
(b) Geopotential height at 500 hPa (contours) and anomaly (shading). The contour interval is 60 m.

JMA's Seasonal Ensemble Prediction System

JMA operates a seasonal Ensemble Prediction System (EPS) using the Coupled atmosphere-ocean General Circulation Model (CGCM) to make seasonal predictions beyond a one-month time range. The EPS produces perturbed initial conditions by means of a combination of the initial perturbation method and the lagged average forecasting (LAF) method. The prediction is made using 51 members from the latest six initial dates (nine members are run every five days). Details of the prediction system and verification maps based on 30-year hindcast experiments (1979 – 2008) are available at http://ds.data.jma.go.jp/tcc/tcc/products/model/.

Cold Season Outlook for Winter 2013/2014 in Japan

In winter 2013/2014, mean temperatures are likely to be near or below normal, both with 40% probability, in northern, eastern and western Japan. Cold-season precipitation amounts are expected to be near or above normal, both with 40% probability, on the Sea of Japan side of northern and eastern Japan, and to be near or below normal, both with 40% probability, on the Pacific side of eastern and western Japan.

1. Outlook summary

JMA issued its outlook for the coming winter over Japan in September and updated it in October. According to the outlook, mean temperatures in winter 2013/2014 are likely to be near or below normal, both with 40% probability, in northern, eastern and western Japan (Figure 8). Cold season precipitation amounts are likely to be near or above normal, both with 40% probability, on the Sea of Japan side of northern and eastern Japan, and to be near or below normal, both with 40% probability, on the Pacific side of eastern and western Japan (Figure 9). Snowfall amounts are expected to be near or above normal, both with 40% probability, on the Sea of Japan side of northern, eastern and western Japan.

2. Outlook background

JMA's coupled global circulation model predicts that SSTs will be above normal in the western tropical Pacific and near normal in the central and eastern tropical Pacific and in the tropical Indian Ocean during the coming winter. In association with SST anomaly patterns, convective activity is predicted to be stronger than normal in the western tropical Pacific.

In the upper troposphere, anti-cyclonic circulation anomalies are predicted from the southeastern part of the Asian Continent to the East China Sea, representing a subtropical jet stream shift northward in these areas and a shift southward over Japan. In association with the southward meandering of the jet stream over Japan, the Aleutian Low is predicted to be stronger than normal near the country, suggesting a stronger-than-normal winter monsoon in the area.

There is almost no signal showing that the Arctic Oscillation (AO) will prevail, and the model does not have sufficient capability to predict the AO accurately. Accordingly, the tendency of the AO is not taken into consideration in this forecast.

Considering all the above, near- or below-normal temperatures are expected during winter in Japan except in Okinawa/Amami.

(Takafumi Umeda, Climate Prediction Division)

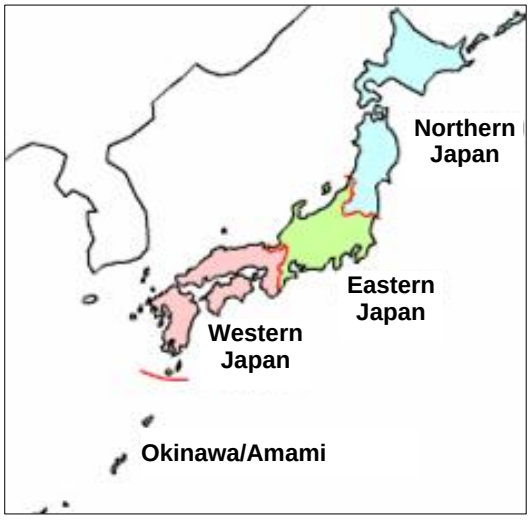

Category	−	0	+
Northern Japan	40	40	20
Eastern Japan	40	40	20
Western Japan	40	40	20
Okinawa and Amami	40	30	30

(Category −: below normal, 0 : normal, + : above normal, Unit: %)

Figure 8 Outlook for winter 2013 temperature probability in Japan

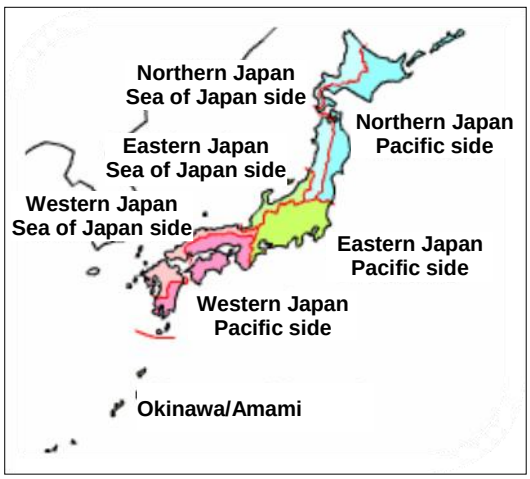

Category		−	0	+
Northern Japan	Sea of Japan side	40	30	30
	Pacific side	40	30	30
Eastern Japan	Sea of Japan side	40	30	30
	Pacific side	40	30	30
Western Japan	Sea of Japan side	30	40	30
	Pacific side	30	40	30
Okinawa and Amami		20	40	40

(Category −: below normal, 0 : normal, + : above normal, Unit: %)

Figure 9 Outlook for winter 2013 precipitation probability in Japan

Summary of the 2013 Asian Summer Monsoon

1. Precipitation and temperature

Four-month total precipitation amounts based on CLIMAT reports covering the monsoon season (June – September) were more than 160% of the normal from northeastern China to eastern Mongolia, around northern China, in eastern and central Kazakhstan, in northern and southern Pakistan, from western China to central India, and in southern Indonesia. The corresponding values were less than 60% of the normal around southeastern South Korea and in parts of eastern and northwestern China (Figure 10). The amounts were mostly consistent with the distribution of outgoing longwave radiation (OLR) anomalies (Figure 12).

Extremely heavy precipitation was seen from eastern India to Pakistan in June, from the Tohoku region of Japan to central China in July, and from northeastern China to eastern Kazakhstan in August. In contrast, extremely light precipitation was seen around the Kyushu region of Japan in July (figures not shown).

Four-month mean temperatures for the same period were more than 1°C above normal from Japan to South Korea and around eastern to central and western China, and were more than 1°C below normal around eastern Mongolia, northeastern Kazakhstan and central India (Figure 11).

It was reported that heavy rains caused more than 600 confirmed fatalities and 5,700 presumed fatalities in India as well as more than 50 fatalities in Nepal in June. It was also reported that heavy rain caused more than 200 fatalities in Pakistan and more than 60 in Afghanistan in August.

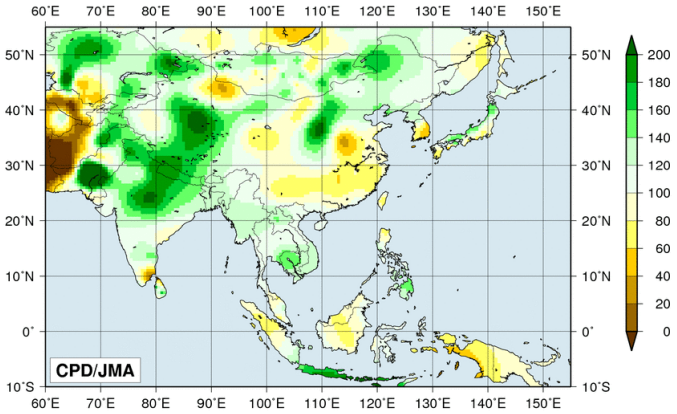

Figure 10 Four-month precipitation ratios (%) from June to September 2013
The base period for normal is 1981 – 2010.

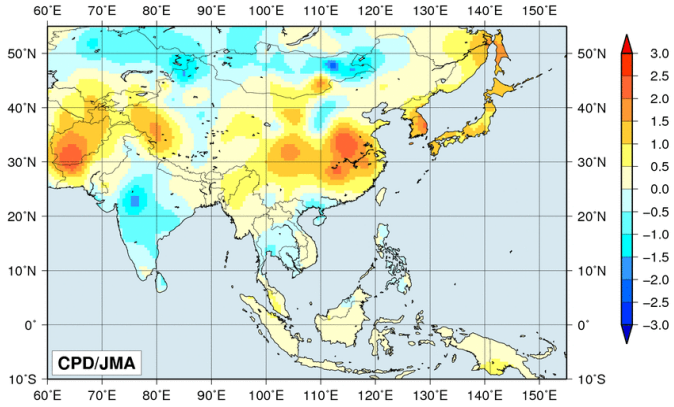

Figure 11 Four-month mean temperature anomalies (°C) from June to September 2013
The base period for normal is 1981 – 2010.

2. Tropical cyclones

During the monsoon season, 21 tropical cyclones (TCs) of tropical storm (TS) intensity or higher formed over the western North Pacific (Table 1). This was higher than the 1981 – 2010 average of 16.0. A total of 6 among these 21 passed around the East China Sea and approached or hit China or Japan, while 8 TCs approached or hit southern China or Viet Nam via the South China Sea. Two TCs also hit the main islands of Japan.

Typhoon Utor caused more than 10 fatalities in Viet Nam and 60 in China, and Typhoon Usagi caused more than 30 fatalities in China.

Note: Disaster information is based on reports by governmental organizations (China and Pakistan), OCHA and IFRC.

Table 1 Tropical cyclones forming over the western North Pacific from June to September 2013

Number ID	Name	Date (UTC)	Category[1)]	Maximum wind[2)] (knots)
T1303	Yagi	6/8 – 6/12	TS	45
T1304	Leepi	6/18 – 6/20	TS	40
T1305	Bebinca	6/20 – 6/24	TS	40
T1306	Rumbia	6/28 – 7/2	STS	50
T1307	Soulik	7/8 – 7/13	TY	100
T1308	Cimaron	7/17 – 7/18	TS	40
T1309	Jebi	7/31 – 8/3	STS	50
T1310	Mangkhut	8/6 – 8/7	TS	40
T1311	Utor	8/9 – 8/15	TY	105
T1312	Trami	8/18 – 8/22	STS	60
T1313	Pewa	8/18 – 8/24	STS	55
T1314	Unala	8/19 – 8/19	TS	35
T1315	Kong-Rey	8/26 – 8/29	STS	55
T1316	Yutu	9/1 – 9/1	TS	35
T1317	Toraji	9/1 – 9/3	STS	50
T1318	Man-Yi	9/13 – 9/16	TY	65
T1319	Usagi	9/16 – 9/23	TY	110
T1320	Pabuk	9/21 – 9/26	STS	60
T1321	Wutip	9/27 – 9/30	TY	65
T1322	Sepat	9/30 – 10/2	TS	40
T1323	Fitow	9/30 – 10/7	TY	75

Note: Based on information from the RSMC Tokyo-Typhoon Center.
1) Intensity classification for tropical cyclones
TS: Tropical storm, STS: Severe tropical storm, TY: Typhoon
2) Estimated maximum 10-minute mean wind

3. Monsoon activity and atmospheric circulation

Convective activity (inferred from OLR) averaged for June – September 2013 was enhanced over large parts of the Asian summer monsoon region including northwestern India, the Bay of Bengal, the South China Sea and the area around the Maritime Continent (Figure 12). According to OLR indices (Table 2), convective activity averaged over the Bay of Bengal and in the vicinity of the Philippines (both core areas of monsoon-related active convection) was enhanced throughout the summer monsoon season, especially in June, July and September.

In the upper troposphere, the Tibetan High was pronounced as a whole and extended toward central China and Japan (Figure 13 (a)). In the lower troposphere, a monsoon trough was prominent from the Arabian Sea to the South China Sea, and westerly winds were stronger than normal from the Arabian Sea to the Bay of Bengal (Figure 13 (b)). Easterly vertical shear over the North Indian Ocean and southern Asia was stronger than normal throughout the monsoon season (Figure 14). These characteristics of anomalous circulation indicate enhanced large-scale circulation related to the monsoon. The Pacific High in the lower troposphere was significantly extended to southern China and Japan, bringing hot summer conditions there (Figure 13 (b)).

References

Webster, P. J. and S. Yang, 1992: Monsoon and ENSO: Selectively interactive systems. *Quart. J. Roy. Meteor. Soc.*, **118**, 877 – 926.

(Sections 1 and 2: Kazuyoshi Yoshimatsu, 3: Hiroshi Ohno, Tokyo Climate Center)

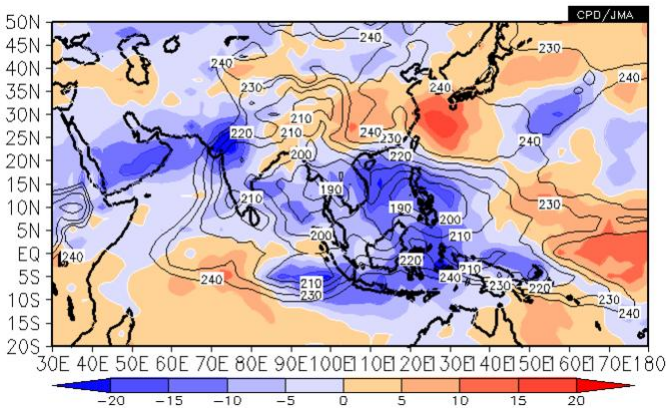

Figure 12 Four-month mean outgoing longwave radiation (OLR) and its anomaly for June – September 2013
The contours indicate OLR at intervals of 10 W/m^2, and the color shading denotes OLR anomalies from the normal (i.e., the 1981 – 2010 average). Negative (cold color) and positive (warm color) OLR anomalies show enhanced and suppressed convection compared to the normal, respectively. Original data provided by NOAA.

Table 2 Summer Asian Monsoon OLR Index (SAMOI) values observed from May to October 2013
Asian summer monsoon OLR indices (SAMOI) are derived from OLR anomalies from May to October. SAMOI (A), (N) and (W) indicate the overall activity of the Asian summer monsoon, its northward shift and its westward shift, respectively. SAMOI definitions are as follows: SAMOI (A) = (-1) × (W + E); SAMOI (N) = S – N; SAMOI (W) = E – W. W, E, N and S indicate area-averaged OLR anomalies for the respective regions shown in the figure on the right normalized by their standard deviations.

	Summer Asian Monsoon OLR Index (SAMOI)		
	SAMOI (A): Activity	SAMOI (N): Northward-shift	SAMOI (W): Westward-shift
May 2013	0.8	-1.2	1.4
Jun. 2013	1.3	-0.1	-0.3
Jul. 2013	1.8	-0.7	0.5
Aug. 2013	0.9	0.1	-0.9
Sep. 2013	1.6	0.2	-0.1
Oct. 2013	0.4	1.4	0.2

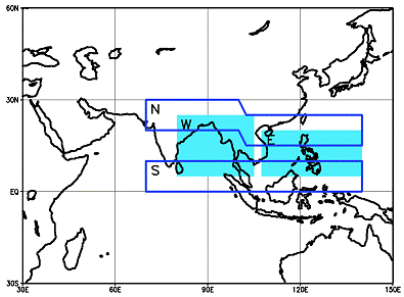

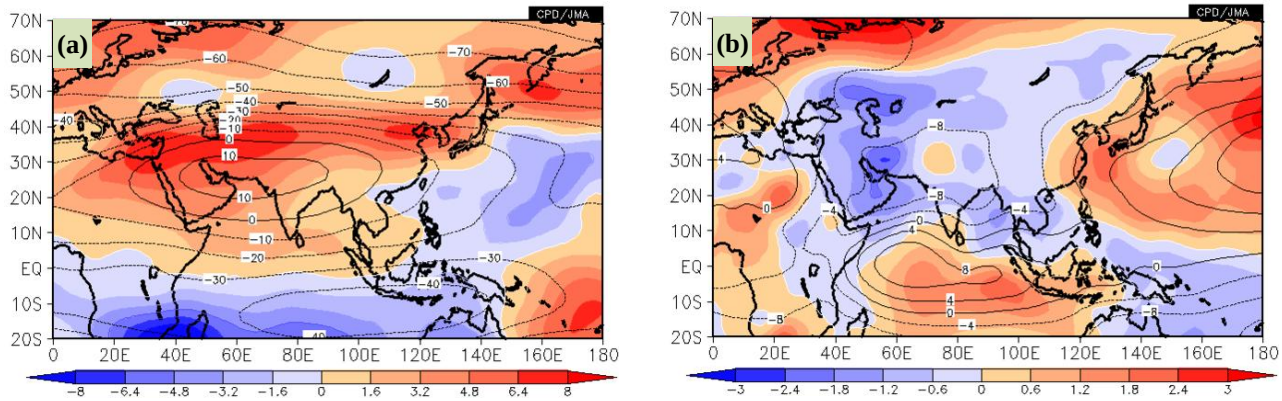

Figure 13 Four-month mean stream function and its anomaly for June – September 2013
(a) The contours indicate the 200-hPa stream function at intervals of 10 × 10^6 m^2/s, and the color shading indicates 200-hPa stream function anomalies from the normal. (b) The contours indicate the 850-hPa stream function at intervals of 4 × 10^6 m^2/s, and the color shading indicates 850-hPa stream function anomalies from the normal. The base period for the normal is 1981 – 2010. Warm (cold) shading denotes anticyclonic (cyclonic) circulation anomalies in the Northern Hemisphere, and vice-versa in the Southern Hemisphere.

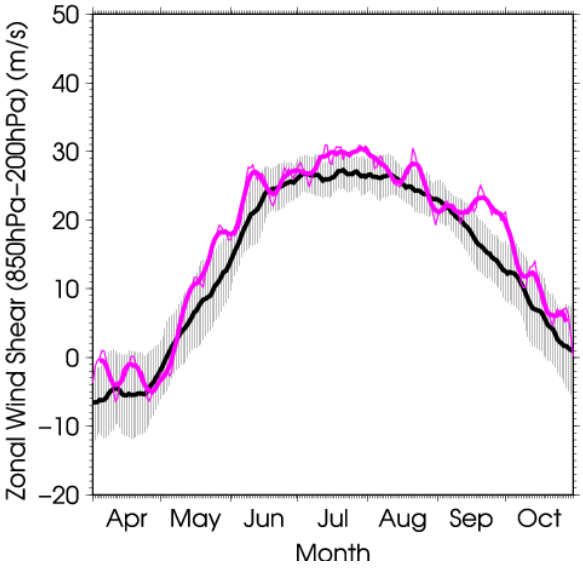

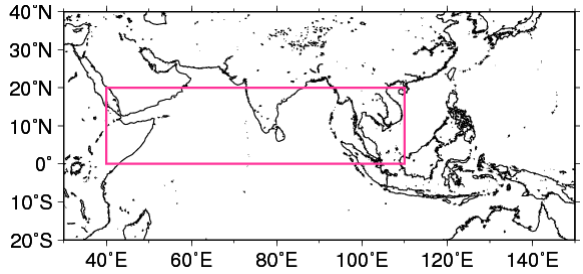

Figure 14 Time-series representation of the zonal wind shear index between 200-hPa and 850-hPa averaged over the North Indian Ocean and southern Asia (pink rectangle in the bottom figure: equator – 20°N, 40°E – 110°E)

The zonal wind shear index is calculated after Webster and Yang (1992). The thick and thin pink lines indicate seven-day running mean and daily mean values, respectively. The black line denotes the normal (i.e., the 1981 – 2010 average), and the gray shading shows the range of the standard deviation calculated for the time period of the normal.

Extreme summer conditions in Japan in 2013

Japan experienced extreme summer (June – August) conditions in 2013, with severe heat (especially in western parts), wetness in the Tohoku region and on the Sea of Japan side of its main islands, and dryness on the Pacific side of its main islands and in Okinawa/Amami. This report summarizes the related surface climate characteristics, atmospheric circulation and primary factors contributing to the extreme conditions observed. These primary factors were clarified based on investigation by JMA's Advisory Panel on Extreme Climatic Events[1].

Note: JRA/JCDAS (Onogi et al. 2007) atmospheric circulation data and COBE-SST (JMA 2006) sea surface temperature (SST)/sea ice concentration data were used for this investigation. The outgoing longwave radiation (OLR) data referenced to infer tropical convective activity were originally provided by the National Oceanic and Atmospheric Administration (NOAA). The base period for the normal is 1981 – 2010. The term "anomaly" as used in this report refers to deviation from the normal. Collection of the area-averaged statistical data referenced here began in 1946. Figure 15 shows a regional breakdown of Japan.

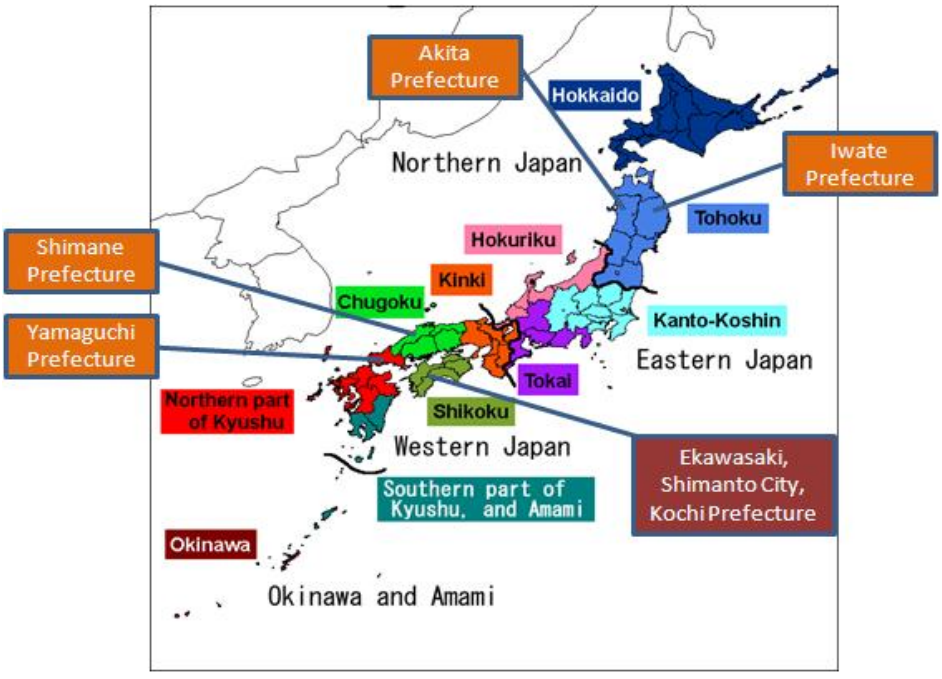

Figure 15 Climatological regions of Japan

The country has four divisions (northern, eastern, western Japan and Okinawa/Amami) and eleven subdivisions (Hokkaido, Tohoku, Kanto-koshin, Hokuriku, Tokai, Kinki, Chugoku, Shikoku, northern Kyushu, southern Kyushu and Okinawa). The map also shows the four prefectures and the observation station referred to in this report.

[1] The Advisory Panel, consisting of prominent experts on climate science from universities and research institutes, was established in June 2007 by JMA to investigate extreme climate events based on up-to-date information and findings.

1. Climatic characteristics

Japan experienced hot summer conditions across the country in 2013 (Figure 16). In particular, the mean summer temperature averaged over western Japan was 1.2°C above normal, which is the highest on record for the season since 1946 (Table 3). The corresponding figure for eastern Japan was 1.1°C above normal (the third highest), and that for Okinawa/Amami was 0.7°C above normal (the second highest). Temperatures were high on the Pacific side of eastern and western Japan around August 10 (Figure 17). In particular, the country's highest-ever temperature of 41.0˚C was recorded on August 12 at Ekawasaki Station in Shimanto City, Kochi Prefecture. Record-high daily maximum temperatures were seen at as many as 143 observation stations. Daily minimum temperatures were also quite high in many places, with 93 stations observing record-high values.

Tohoku and the Sea of Japan side of Japan's main island experienced wet conditions (Figure 16). In particular, frequent heavy precipitation was observed in the Tohoku region. The monthly precipitation ratio to the normal averaged over Tohoku for July was 182% (the highest on record for the month), and the three-month precipitation ratio to the normal averaged over the region for summer was 151% (the fourth highest on record for the season). Precipitation of unprecedented intensity was also observed in the prefectures of Yamaguchi, Shimane, Akita and Iwate. The number of events with extreme precipitation (exceeding 80 mm per hour) observed during summer[2] was the third highest since 1976 (Figure 18).

Some areas on the Pacific side of eastern and western Japan and parts of Okinawa/Amami experienced dry conditions (Figure 16). The monthly precipitation ratio to the normal averaged over southern Kyushu and Amami for July was 11% (the lowest on record for the month), and the seasonal precipitation ratio to the normal averaged over Tokai for the summer was 64% (the third lowest on record for the season).

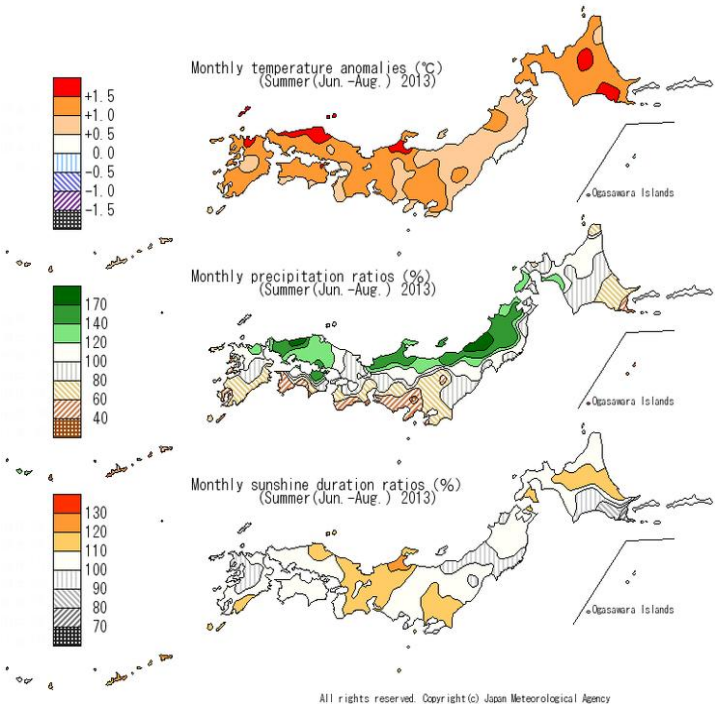

Figure 16 Temperature anomalies, precipitation ratios and sunshine duration ratios for summer (June – August) 2013

Table 3 Ranking: regional average of seasonal temperature anomalies for summer (June – August)

	1st	2nd	3rd	2013
Northern Japan	+2.2°C (2010)	+1.9°C (1978)	+1.5°C (1999/others)	+1.0°C Joint 10th
Eastern Japan	+1.5°C (2010)	+1.3°C (1994)	+1.1°C (2013/others)	+1.1°C Joint 3rd
Western Japan	+1.2°C (2013)	+1.1°C (1994)	+0.9°C (2004)	+1.2°C 1st
Okinawa/ Amami	+0.8°C (1991)	+0.7°C (2013/others)	–	+0.7°C Joint 2nd

* Since 1946

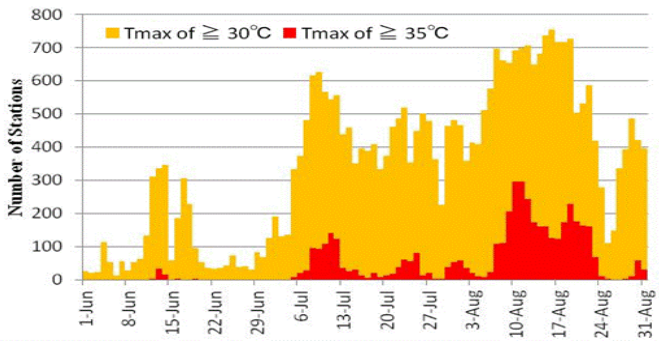

Figure 17 Time-series representations of the number of stations where daily maximum temperatures of 30°C or above (Tmax ≥ 30°C) and 35°C or above (Tmax ≥ 35°C) were observed from 1 June to 31 August, 2013

Based on data from 927 surface meteorological stations in Japan

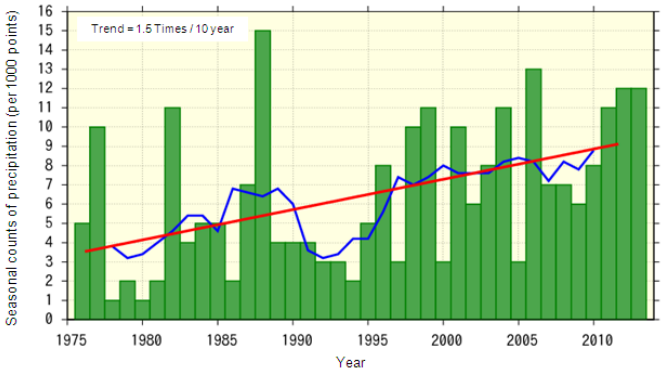

Figure 18 Number of summer (June – August) events with precipitation exceeding 80 mm/hour from 1976 to 2013 (per 1,000 Automated Meteorological Data Acquisition System (AMeDAS) points)

The green bars indicate values for each year. The blue line indicates the five-year running mean, and the straight red line indicates the long-term linear trend.

[2] The number of precipitation events is expressed on a per-1,000-station basis for precipitation per hour (with observations made on the hour every hour) since 1976 so that the data used are obtained using a uniform method.

2. Characteristic atmospheric circulation causing Japan's extreme summer conditions

(1) General characteristics observed in July and August 2013

The northwestern Pacific High (a lower-level high-pressure system) and the Tibetan High (an upper-level high-pressure system), which govern Japan's summer climate, were enhanced during July and August 2013 (Figure 19). In particular, the Pacific High continued to expand westward and predominantly developed over Okinawa/Amami and western Japan. The country experienced hot conditions nationwide, especially in its western part, due to these enhanced high-pressure systems. SSTs around Japan in August were significantly higher than normal due in part to predominant sunny conditions associated with the high-pressure systems (Figure 20).

Convective activity was significantly enhanced over large parts of the Asian summer monsoon region (South and Southeast Asia) (Figure 21) in association with SST anomaly patterns in the Pacific (above-normal around Indonesia and the Philippines, and below-normal in the equatorial central-eastern Pacific) (Figure 22). This heightened convective activity contributed to the enhancement of the Pacific High around Japan and the Tibetan High.

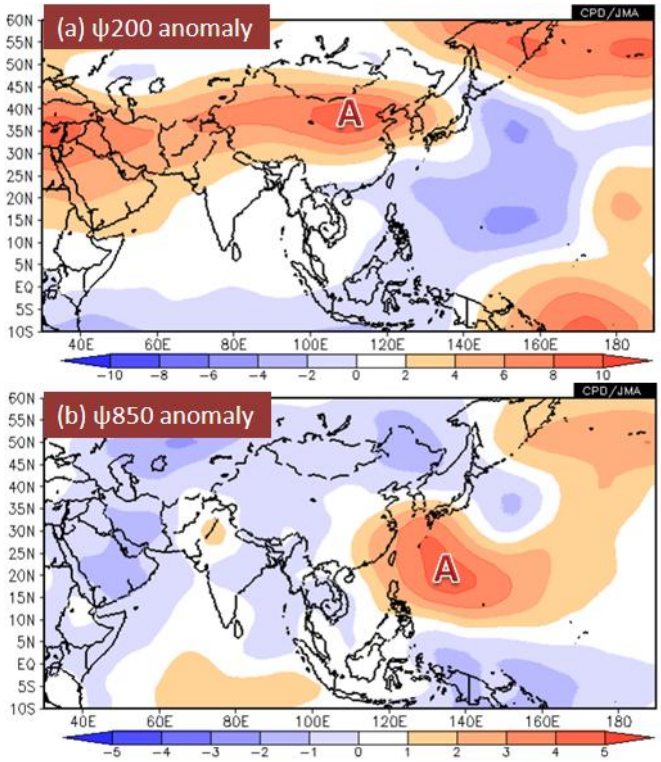

Figure 19 Two-month mean 200-hPa and 850-hPa stream function anomalies (July and August 2013)
The shading shows (a) 200-hPa and (b) 850-hPa stream function anomalies at intervals of 2×10^6 m^2/s and 1×10^6 m^2/s, respectively. "A" marks the center of anticyclonic circulation anomalies.

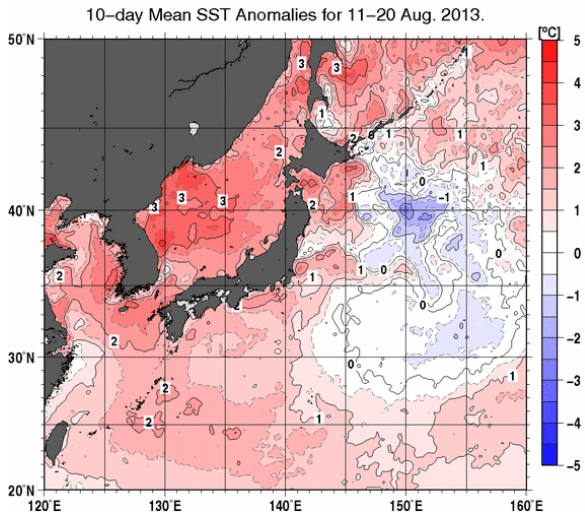

Figure 20 10-day mean sea surface temperature (SST) anomalies (11 – 20 August 2013)
The contour interval is 0.5°C. Numbers expressing SST anomalies are preliminary values.

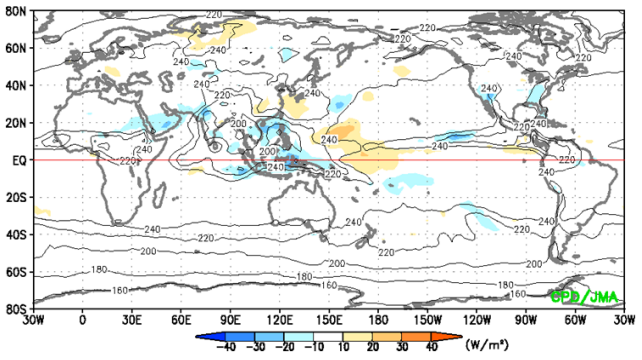

Figure 21 Two-month mean outgoing longwave radiation (OLR) and anomalies (July and August 2013)
The contours indicate OLR at intervals of 20 W/m^2 (shown for 240 W/m^2 or less). The shading shows OLR anomalies.

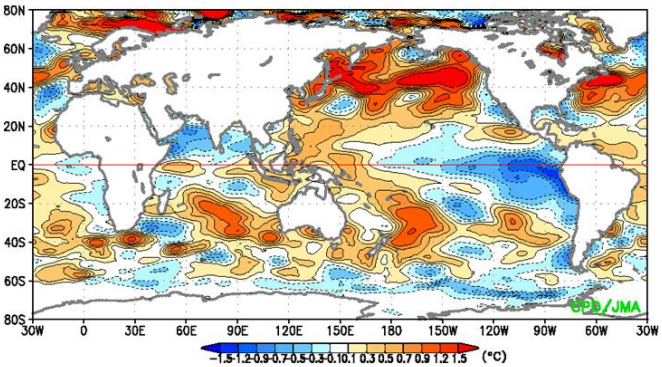

Figure 22 Two-month mean sea surface temperature (SST) anomalies (July and August 2013)
Warm (cold) coloring indicates positive (negative) SST anomalies.

(2) Primary factors contributing to the heavy rain and dry conditions observed in July and August 2013

The northwestern Pacific High expanded northward to the Pacific side of western and eastern Japan in early July, and remained centered over areas to the south of Japan and Okinawa/Amami in its enhanced form. Warm moist air continued to flow over the Sea of Japan along the western and northern periphery of the Pacific High, contributing to heavy rain in Tohoku and on the Sea of Japan side of the country (Figure 23). Upper cold air occasionally flowed over Japan in association with the southward meandering of westerly winds (the subtropical jet stream), contributing to heavy rain brought by unstable atmospheric conditions. Significantly above-normal SSTs in the Sea of Japan may have contributed to the transportation of wet air masses over its surface to Tohoku with minimal demoisturization. Dry conditions in Okinawa/Amami and on the Pacific side of western and eastern Japan persisted throughout July and August due to the presence of the prevailing high-pressure systems.

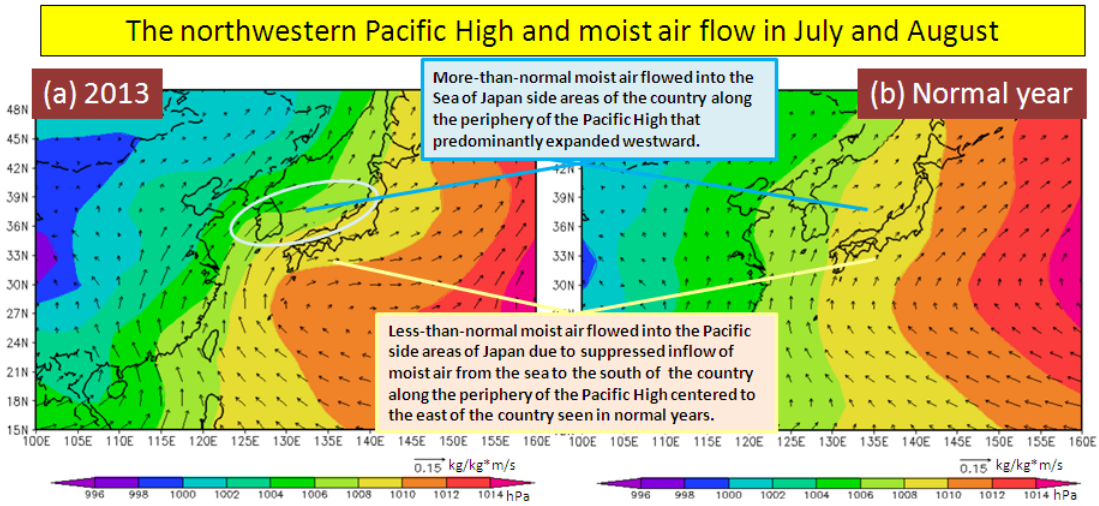

Figure 23 Pacific High and moist air flow around Japan (1 July – 27 August)
The panels on the left and right show (a) 2013 and (b) the normal, respectively. The shading indicates sea level pressure, and the arrows show 925-hPa water vapor flux.

(3) Primary factors contributing to the extremely hot conditions observed in mid-August 2013

The northwestern Pacific High was enhanced over Okinawa/Amami and western and eastern Japan, and the Tibetan High expanded to the main islands of the country in line with the northward meandering of upper-level westerly winds (the subtropical jet stream). Surface temperatures in Japan increased due to predominant sunny conditions and downward flow in association with these high-pressure systems. In addition, significantly warmer-than-normal air was advected over eastern China and the East China Sea to the main islands of Japan along the northern periphery of the enhanced northwestern Pacific High (Figure 24). Northerly winds also prevailed over the Pacific side of western and eastern Japan, preventing sea winds from blowing into these areas. The resulting long sunshine durations and weak sea winds exacerbated the effects of urbanization (e.g., the heat island phenomenon) on the Pacific side of Japan, thereby keeping nighttime and early-morning temperatures relatively high.

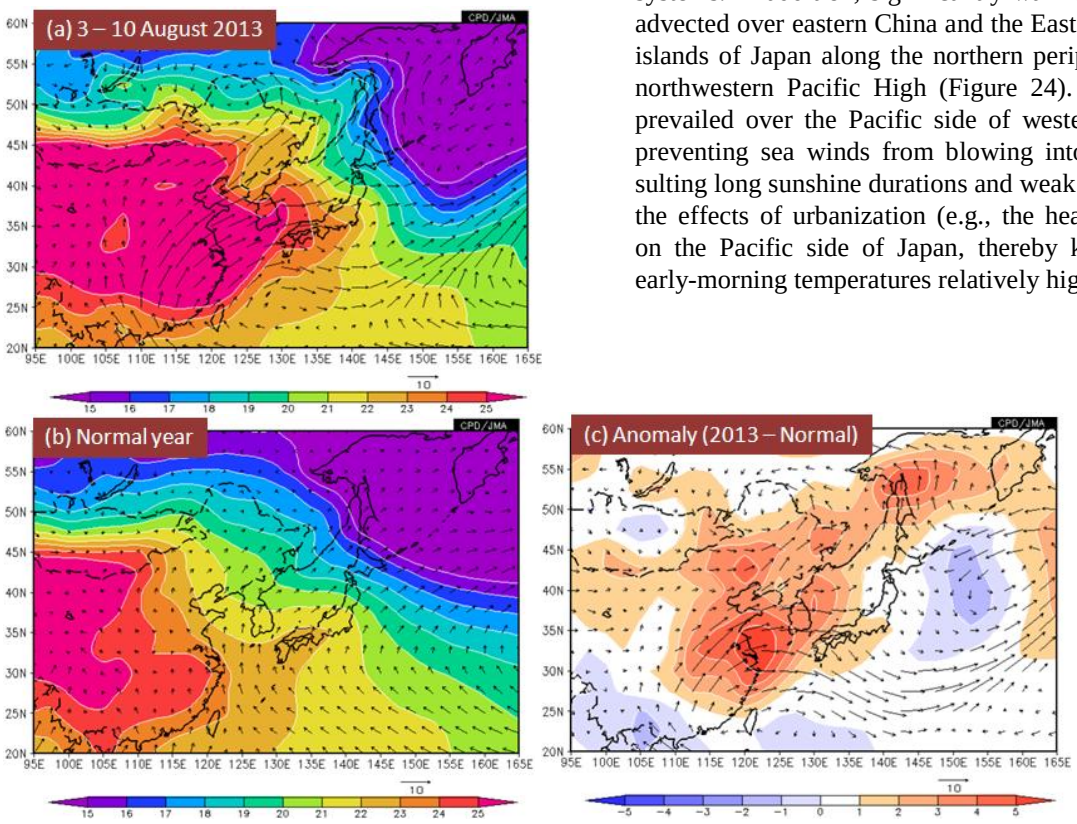

Figure 24 Eight-day mean 925-hPa wind vectors and temperatures (3 – 10 August)
The top-left, top-right and bottom-left panels show (a) 2013, (b) the normal and (c) anomalies, respectively. The arrows show wind vectors (m/s), and the shading indicates temperatures (°C).

(4) Long-term temperature trends

Based on observational records from stations considered to have been affected to a lesser extent by local urbanization, it is virtually certain that the summer mean surface temperature over Japan has risen since 1898 (Figure 25) and that the annual number of days with maximum temperatures of 35°C or above has increased since 1931 (Figure 26). These long-term trends can be largely attributed to global warming caused by increased concentrations of greenhouse gases such as CO_2.

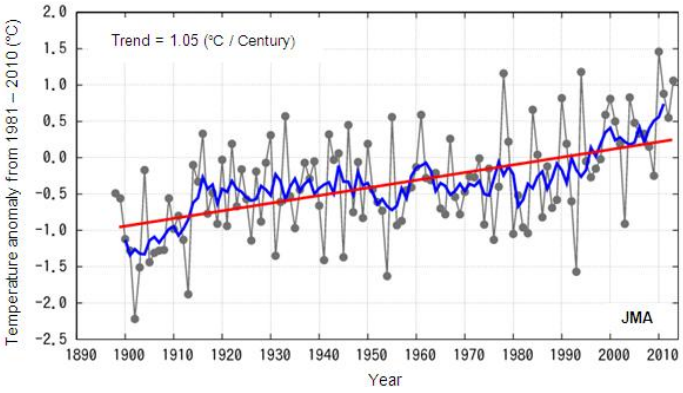

Figure 25 Seasonal surface temperature anomalies in summer (June – August) from 1898 to 2013 in Japan

The thin black line with dots indicates seasonal surface temperature anomalies at 17 stations considered to have been affected to a lesser extent by local urbanization for each year. The blue line indicates the five-year running mean, and the red line indicates the long-term linear trend. Anomalies are deviations from the baseline (the 1981 – 2010 average).

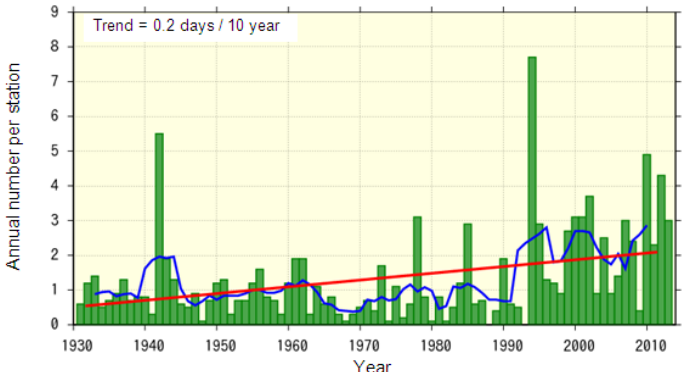

Figure 26 Annual number of days with maximum temperatures of 35°C or above from 1931 to 2013

The green bars indicate values for each year. The blue line indicates the five-year running mean, and the straight red line indicates the long-term linear trend. JMA selected 15 stations considered to have been affected to a lesser extent by local urbanization for these data. The figure for 2013 is a preliminary value as of 1 September.

3. Summary

In July and August 2013, western and other parts of Japan experienced extremely hot summer conditions due to enhancement of the Pacific High and the Tibetan High. Areas on the Sea of Japan side often experienced heavy precipitation due to warm moist flow around the periphery of the Pacific High, which expanded westward. The enhancement of both highs was mainly due to the wide-area influence of a rather active Asian monsoon resulting from above-normal SSTs around Indonesia and the Philippines and below-normal SSTs in the central and eastern equatorial Pacific. The primary factors considered to have contributed to these extreme conditions are summarized in Figure 27.

(Shotaro Tanaka, Tokyo Climate Center)

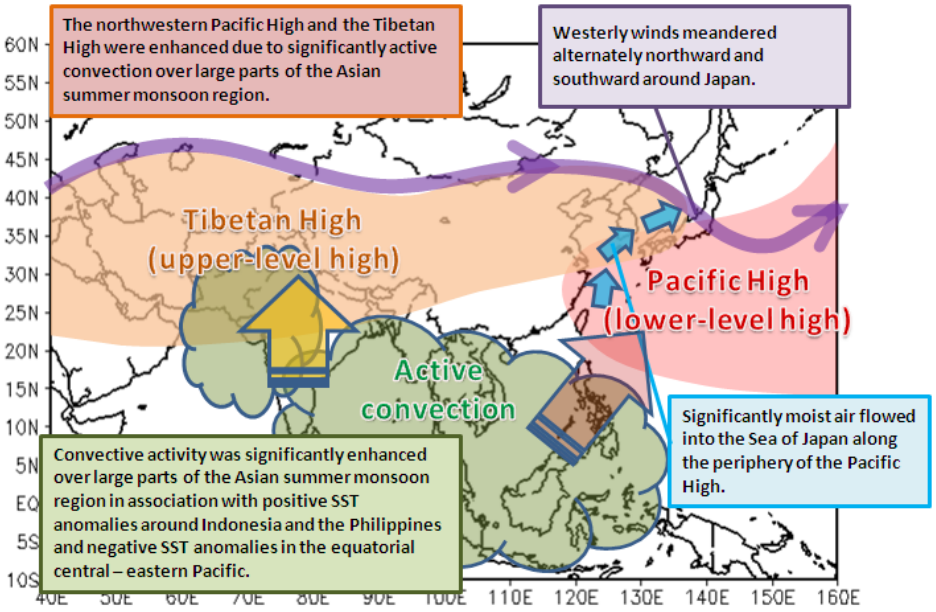

Figure 27 Primary factors contributing to the extreme summer conditions observed in Japan in July and August, 2013

Status of the Antarctic Ozone Hole in 2013

The size of the Antarctic ozone hole in 2013 was equivalent to its average over the last 10 years.

Over the last 30 years, the Antarctic ozone hole has appeared every year in Austral spring with a peak in September or early October. Its scale is generally defined as the area in which the total ozone column is equal to or less than 220 m atm-cm.

According to JMA analysis based on data from National Aeronautics and Space Administration (NASA) satellites, the Antarctic ozone hole in 2013 appeared in mid-August and expanded rapidly from late August to early September, reaching its maximum size for the year on 16 September. At this time it covered 23.4 million square kilometers (see the upper left panel in Figure 28), which is 1.7 times as large as the Antarctic Continent. The scale of the Antarctic ozone hole in 2013 was equivalent to the average over the last 10 years, and its maximum size was comparable to those of 2004 and 2009 (upper right panel). The bottom panels in Figure 28 indicate the progress of this year's ozone hole.

The ozone layer acts as a shield against ultraviolet radiation, which can cause skin cancer. The ozone hole first appeared in the early 1980s and reached its maximum size of 29.6 million square kilometers in 2000. The amount of ozone in the Antarctic region is expected to return to pre-1980 levels in the late 21st century according to WMO/UNEP Scientific Assessment of Ozone Depletion: 2010. Close observation of the ozone layer on a global scale (including that over the Antarctic region) remains important.

(Atsuya Kinoshita, Ozone Layer Monitoring Office)

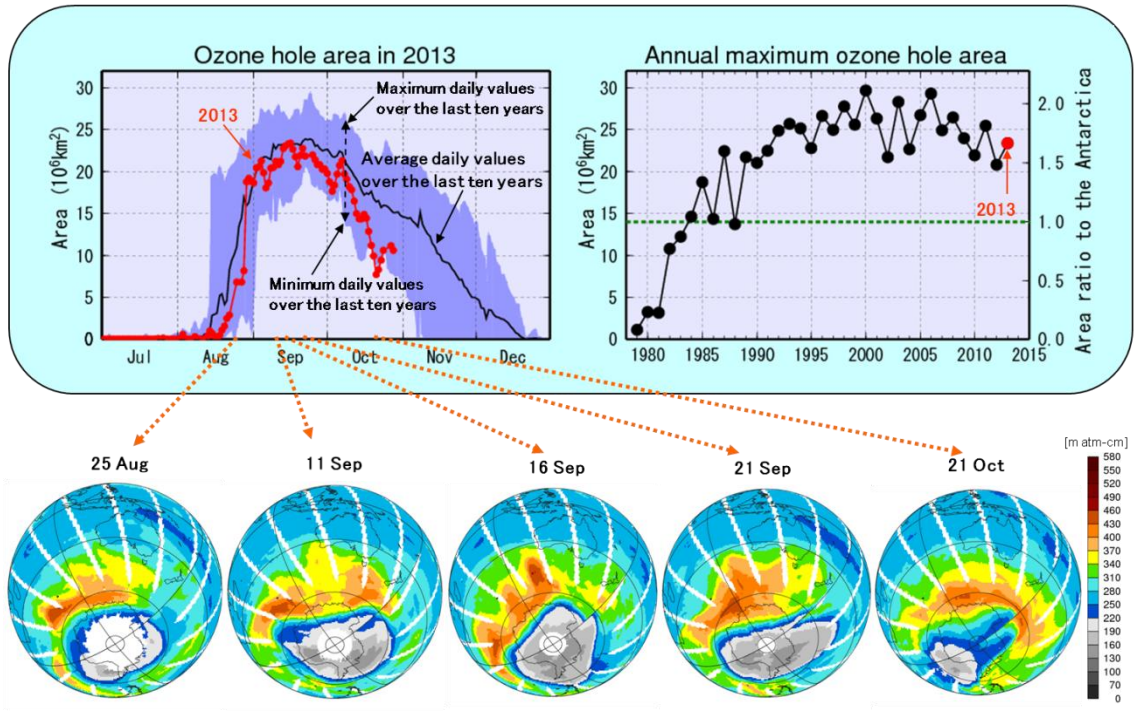

Figure 28 Antarctic ozone hole characteristics
Upper left: Time-series representation of the daily ozone-hole area for 2013 (red line) and the 2003–2012 average (black line). The blue shading area represents the range of daily minima and daily maxima over the past 10 years. Upper right: Interannual variability in the annual maximum ozone-hole area. Bottom: Snapshots of total column ozone distribution on selected days in 2013; the ozone hole is shown in gray. These panels are based on data from NASA satellite sensors of the total ozone mapping spectrometer (TOMS) and ozone monitoring instrument (OMI).

TCC Training Seminar on Seasonal Prediction Products

JMA's Tokyo Climate Center (TCC) assists National Meteorological and Hydrological Services (NMHSs) in improving their climate services. The Center's two major activities in this regard involve providing basic climate data and products to NMHSs through its website and assisting with capacity development at NMHSs in the Asia-Pacific region. TCC holds annual training seminars as part of capacity development activities related to its role as an RCC in the WMO RA II area. In addition to running annual training seminars, it arranges expert visits to and hosts visitors from NMHSs to support discussions on climate services and the effective transfer of technology.

In 2013, TCC held the Training Seminar on Seasonal Prediction Products from 11 to 15 November at JMA Headquarters in Tokyo. The event was attended by 16 experts from NMHSs in Bangladesh, Cambodia, Hong Kong (China), Indonesia, Lao People's Democratic Republic, Malaysia, Mongolia, Myanmar, Nepal, Papua New Guinea, the Philippines, Sri Lanka, Thailand and Viet Nam. The seminar focused on familiarizing the participants with the outputs of JMA's numerical prediction model and improving their skills in generating seasonal prediction products using statistical downscaling methods. The teaching involved lectures and practical exercises using data, products and a web-based application tool available on the TCC website as well as in-situ observation data brought by participants. At the end of the seminar, all participants gave presentations on seasonal prediction in their own countries and engaged in fruitful discussions with lecturers and participants.

The content of the lectures is available on the TCC website (http://ds.data.jma.go.jp/tcc/tcc/library/library2013.html).

(Teruko Manabe, Tokyo Climate Center)

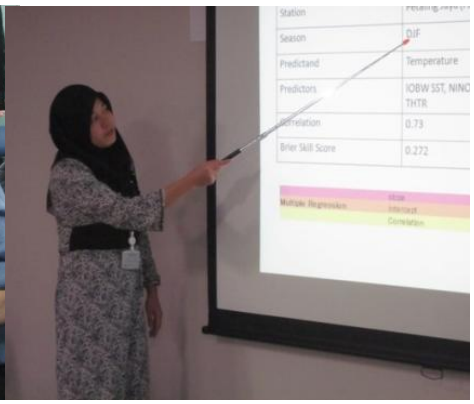

Any comments or inquiry on this newsletter and/or the TCC website would be much appreciated. Please e-mail to tcc@met.kishou.go.jp.

(Editors: Teruko Manabe, Ryuji Yamada and Kenji Yoshida)

Tokyo Climate Center (TCC), Japan Meteorological Agency
Address: 1-3-4 Otemachi, Chiyoda-ku, Tokyo 100-8122, Japan
TCC Website: http://ds.data.jma.go.jp/tcc/tcc/index.html